Chinese Chemical Letters 35 (2024) 108136

Contents lists available at ScienceDirect

Chinese Chemical Letters

journal homepage: www.elsevier.com/locate/cclet

Design and synthesis of tri-substituted pyrimidine derivatives as bifunctional tumor immunotherapeutic agents targeting both A_{2A} adenosine receptors and histone deacetylases

Ruiquan Liu[a], Wenwen Duan[a], Wenzhong Yan[a], Jinfeng Zhang[a], Jianjun Cheng[a,b,*]

[a] *iHuman Institute, ShanghaiTech University, Shanghai 201210, China*
[b] *School of Life Science and Technology, ShanghaiTech University, Shanghai 201210, China*

ARTICLE INFO

Article history:
Received 11 October 2022
Revised 3 January 2023
Accepted 4 January 2023
Available online 5 January 2023

Keywords:
Bifunctional
A_{2A}AR antagonism
HDAC inhibition
Cancer
Immunotherapy

ABSTRACT

The A_{2A} adenosine receptor (A_{2A}AR) has attracted attention as an emerging immunotherapeutic target with several antagonists being evaluated in clinical trials. However, A_{2A}AR antagonists show limited efficacy as monotherapies. Herein, we communicate our design and synthesis of a novel series of A_{2A}AR/histone deacetylase (HDAC) bifunctional inhibitors, based on the core structure of the A_{2A}AR antagonist **PBF-509**. The new compounds were designed using a pharmacophore-merging strategy and features a tri-substituted pyrimidine core. The binding affinity for A_{2A}AR and inhibitory activity against HDACs of all the new compounds were tested. A number of compounds exhibited nanomolar or subnanomolar activity against both targets and some showed equally potent antiproliferative activity against MC38, CT26 and HCT116 colon cancer lines compared to HDAC inhibitors **SAHA** and **MGCD-0103** *in vitro*. The binding poses of compound **5a** in both A_{2A}AR and HDAC1 were predicted by molecular docking studies. Collectively, these results suggest these tri-substituted pyrimidine derivatives are promising leads for developing A_{2A}AR/HDAC dual-acting compounds as novel antitumor agents.

The development of immunotherapy has been a milestone for the treatment of cancer. Successful immunotherapeutics include checkpoint inhibitors targeting the programmed death-1 (PD-1), programmed death-ligand 1 (PD-L1) and cytotoxic T lymphocyte-associated antigen-4 (CTLA-4). However, tumor has immune escaping mechanisms and the efficacy of existing strategy is limited. Therefore, the development of novel immunotherapeutics targeting alternative immune escaping pathways is urgent.

In the tumor microenvironment (TME), the critical mechanism of tumor immune escape has been shown to be mediated by the accumulation of extracellular adenosine [1,2]. Among the four subtypes of adenosine receptors, the A_{2A}AR has been demonstrated as the major target that mediates the immunosuppressive effects of adenosine in TME, which is highly expressed on multiple T cells and natural killer cells [3–6]. Recently, a number of A_{2A}AR antagonists have been developed and are undergoing extensive evaluations in clinical trials as potential cancer immunotherapies (*e.g.* **PBF-509**) (Fig. 1) [7,8]. However, A_{2A}AR antagonists show limited antitumor effects and are more commonly tested in combination with cytotoxic drugs or other checkpoint inhibitors [7]. From a medicinal chemistry point of view, the design of polypharmacological molecules would be a better alternative to drug combinations, with advantages such as the absence of drug-drug interactions and better patient compliance [9].

The histone deacetylases (HDACs) are validated epigenetic drug targets, and several HDAC inhibitors have been developed as antitumor drugs. Chemical structures of HDAC inhibitors (HDACis), for example vorinostat (**SAHA**) and mocetinostat (**MGCD-0103**), are commonly comprised of three parts: the surface recognition moiety (CAP), a linker group, and the terminal zinc-binding group (ZBG) (Fig. 1). These structural features have made HDACs a popular target for the design of bifunctional antitumor agents. For example, DNMT/HDAC [10,11], EGFR/HDAC [12,13], ErbB/HDAC [14], PI3K/HDAC [15], topisomerase/HDAC [16,17], and JAK/HDAC [18,19], have been reported. In our previous studies, a bifunctional strategy has been used for the design of novel A_{2A}AR/HDAC dual-acting agents, which led to the discovery of potent antitumor agents [20,21]. Recently, based on the clinical agent **PBF-509**, we have initiated another campaign to design novel A_{2A}AR/HDAC dual-acting compounds (Fig. 1).

Among the clinically investigated A_{2A}AR antagonists, **PBF-509** features a relatively low molecular weight (Mw = 305). To ratio-

* Corresponding author.
E-mail address: chengjj@shanghaitech.edu.cn (J. Cheng).

https://doi.org/10.1016/j.cclet.2023.108136
1001-8417/

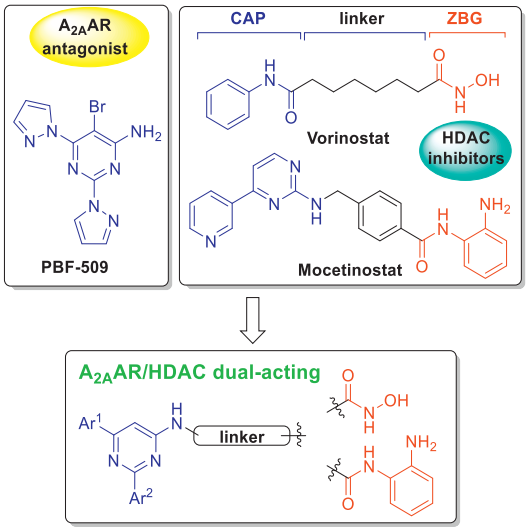

Fig. 1. Structures of the A_{2A}AR antagonist **PBF-509**, HDAC inhibitors vorinostat and mocetinostat, and the design of dual A_{2A}AR/HDAC inhibitors.

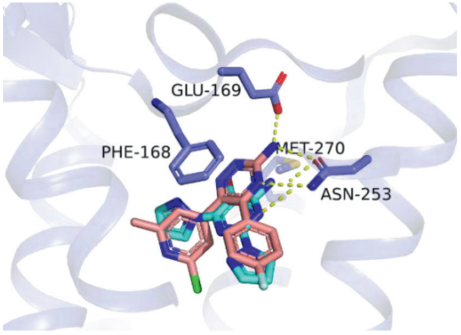

Fig. 2. Binding poses of **PBF-509** in A_{2A}AR predicted by molecular docking. Structure of A_{2A}AR-StaR2-b_{RIL}562 (PDB ID: 6GT3) is shown in pale gray, **AZD-4635** in salmon, and compound **PBF-509** in cyan, respectively. Key residues interacting with **PBF-509** are highlighted. Nitrogen atoms are colored in blue, bromine in firebrick, fluorine in aquamarine and chlorine in green.

nally design bifunctional compounds based on **PBF-509**, we first conducted a molecular docking study using the reported A_{2A}AR-StaR2-b_{RIL}562-AZD-4635 complex structure (PDB ID: 6GT3) [22]. As shown in Fig. 2, the 2-pyrazole substituent of **PBF-509** occupies a hydrophobic cleft at the bottom of the binding pocket. The 6-pyrazole substituent occupies the ribose-binding pocket. The NH_2 group makes an H-bond interaction with the side chain of Asn253$^{6.55}$. In addition, Phe168 on extracellular loop 2 (ECL2) forms π-π stacking interactions with the pyrimidine and 6-pyrazole, and the side chain of Met270$^{7.35}$ makes a hydrophobic interaction from the opposite side. The NH_2 group of **PBF-509** points towards the solvent accessible surface, therefore providing a modification site for incorporating structural elements of HDACis. Based on this NH_2 group, three types of linker groups were designed: amide, urea and carbamate.

PBF-509 was prepared according to reported procedures [23], but coupling reactions of it with aliphatic acids failed to provide amide intermediates. So the bromo group was removed. Variations of the aromatic substituents on the pyrimidine core were incorporated, based on the results from reported structure-activity relationship studies [24–26]. As shown in Scheme 1 (details can be found in Supporting information), starting materials **1a-d** were coupled with a variety of aliphatic acids to produce the key ester intermediates **2a-g**. However, cleavage of the amide bond was

Table 1
A_{2A}AR and HDAC bifunctional activity of designed compounds.[a]

Compound	A_{2A}AR (K_i, nmol/L)	HDAC1 (IC_{50}, nmol/L)	HDAC6 (IC_{50}, nmol/L)
5a	3.7 ± 1.1	0.64 ± 0.06	6.1 ± 1.4
5b	14.3 ± 3.8	2.0 ± 0.7	8.2 ± 1.3
5c	7.9 ± 0.4	0.60 ± 0.07	4.1 ± 0.7
5d	6.8 ± 0.3	5.7 ± 0.5	18.4 ± 7.5
5e	37.1 ± 6.3	17.9 ± 8.8	26.2 ± 5.8
5f	6.7 ± 2.3	6.6 ± 1.2	7.0 ± 2.9
5g	7.8 ± 1.2	8.1 ± 2.7	38.5 ± 1.8
10a	63.9 ± 30.5	6.6 ± 0.4	337.0 ± 216.4
10b	50.0 ± 16.3	6.5 ± 2.0	58.0 ± 19.8
10c	103.3 ± 51.4	3.2 ± 1.9	10.8 ± 3.0
10d	21.2 ± 2.0	1.5 ± 0.7	1.5 ± 0.1
10e	47.6 ± 5.3	7.1 ± 1.2	7.9 ± 1.5
10f	105.8 ± 37.3	7.8 ± 2.0	13.1 ± 4.9
10g	24.5 ± 3.5	3.3 ± 0.3	7.7 ± 0.5
10h	21.0 ± 6.3	4.7 ± 1.0	7.2 ± 0.8
10i	5.9 ± 0.2	1.2 ± 0.1	5.9 ± 1.1
14a	44.1 ± 17.3	132.0 ± 86.3	243.5 ± 36.4
14b	38.4 ± 5.7	13.9 ± 4.3	24.0 ± 7.8
14c	40.6 ± 1.3	1.8 ± 0.6	10.7 ± 2.4
14d	39.8 ± 5.6	25.5 ± 12.8	15.5 ± 3.2
18a	5.0 ± 0.1	0.72 ± 0.01	4.1 ± 0.4
18b	35.5 ± 5.2	2.9 ± 0.4	7.7 ± 0.9
18c	24.9 ± 13.2	3.0 ± 0.7	22.1 ± 7.1
18d	4.0 ± 1.0	0.89 ± 0.19	3.0 ± 0.6
18e	48.0 ± 4.6	2.7 ± 0.3	8.0 ± 2.1
19a	20.5 ± 6.5	9.7 ± 1.0	>10,000
19b	45.4 ± 5.8	54.1 ± 19.2	>10,000
19c	15.6 ± 7.8	122.8 ± 82.9	>10,000
19d	5.1 ± 1.5	56.8 ± 34.1	>10,000
PBF-509	12.0 ± 0.2 [28]	NT	NT
SAHA	NT	14.6 ± 1.4	18.5 ± 6.5

NT: not tested.
[a] Values for $n \geq 2$ reported as the mean ± SEM.

observed when these ester intermediates were treated with aqueous hydroxylamine under basic condition. Therefore, the esters **2a-g** were first hydrolyzed to acids **3a-g** in the presence of LiI and pyridine [27]. Then **3a-g** were coupled with *O*-(tetrahydropyran-2-yl)hydroxylamine to give **4a-g**, and hydroxamic acids **5a-g** were obtained after de-protection of the pyran group (Scheme 1, I).

To synthesize urea- and carbamate-linked compounds, the materials **1a-d** were first coupled with phenyl chloroformate to provide intermediates **6a-d**, then substituted with a variety of amines or alcohols to provide the key ureas **7a-i** and carbamates **11a-d**. These intermediates were then hydrolyzed to provide acids **8a-i** and **12a-d**, coupled with *O*-(tetrahydropyran-2-yl)hydroxylamine, and then hydrolyzed to afford the corresponding hydroxamic acids **10a-i** and **14a-d** (Scheme 1, II and III).

A combination of an urea group and a benzyl linker was also introduced, and the compounds were synthesized according to Scheme 2 (details can be found in Supporting information). The carbamates **6a-d** were converted to ester intermediates **15a-e** and then hydrolyzed to acids **16a-e**. These acids were converted to hydroxamates **18a-e** using similar conditions as described above. Acids **16a-d** were also coupled with *o*-phenylenediamine to afford amide compounds **19a-d**.

As shown in Table 1, most target compounds displayed potent dual-acting activities, with potent A_{2A}AR binding affinity (**PBF-509** as a positive control [28]) and HDAC1/HDAC6 inhibition (**SAHA** as a positive control), respectively. Among the three types of linker groups, amide connection provided the best activity (**10d** *versus* **5c**, **14d**). Regarding the length of the alkyl chain, **5c**, **10d** and **14c** were the best with 6 or 5 carbon chains, while longer or shorter chains showed weaker activity (**5c** *versus* **5a**, **5b**, **5d**; **10d** *versus* **10a**, **10b**, **10c**; **14c** *versus* **14a**, **14b**, **14d**). For ureas, alkyl substitution weakened the activity (**10d** *versus* **10e**, **10f**), and the same was true for aromatic linkers (**18a** *versus* **18e**). For the ZBG group,

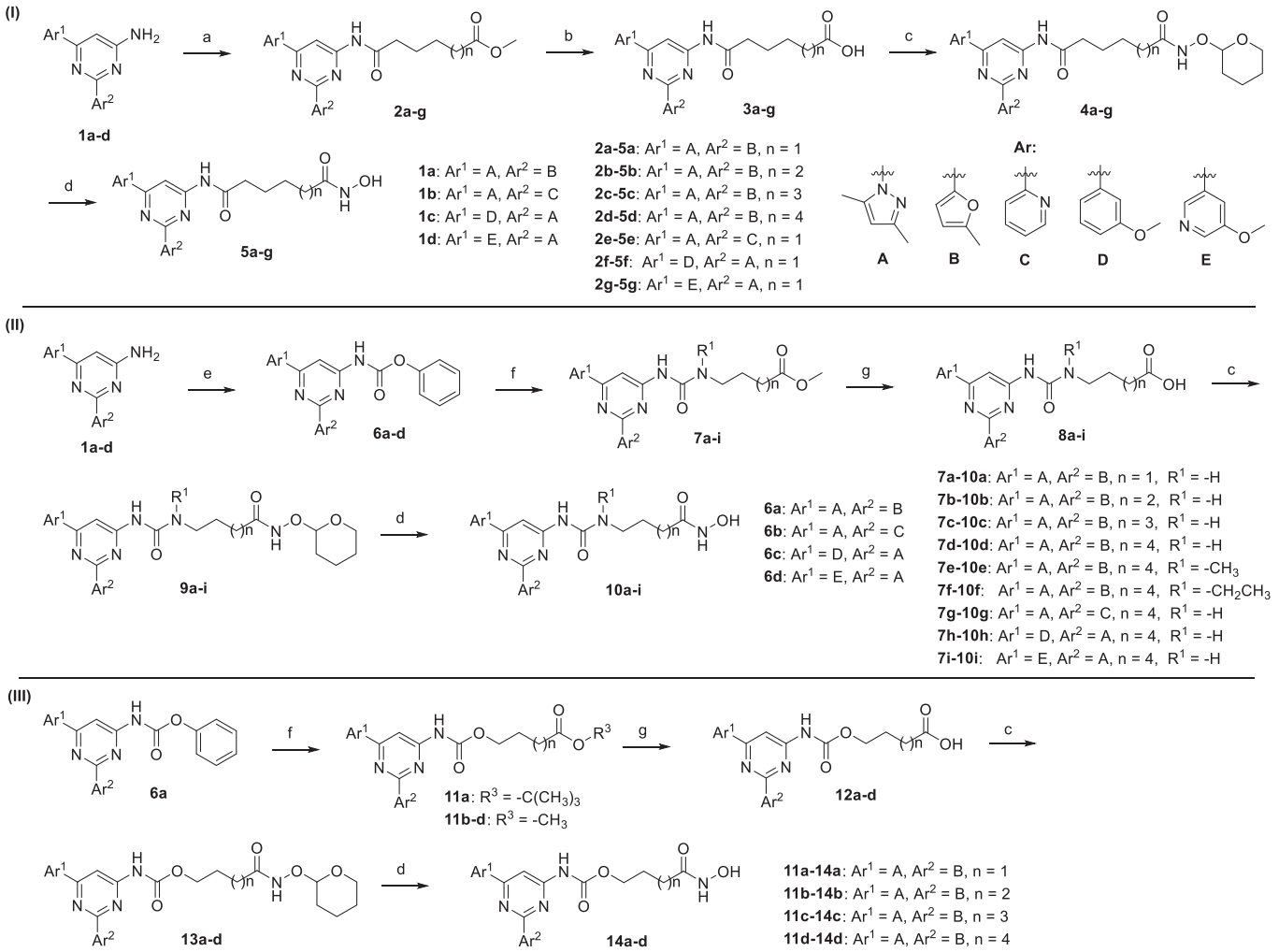

Scheme 1. Synthesis of compounds **5a**-**g**, **10a**-**i** and **14a**-**d**. Reagents and conditions: (a) (i) $SOCl_2$, acid esters, benzotriazole, DCM, r.t., 1 h; (ii) pyridine, DCM, r.t., 12 h; (b) LiI, pyridine, reflux, 12 h; (c) 2-(aminooxy)tetrahydro-2*H*-pyran, HATU, DIPEA, DCM, r.t., 12 h; (d) HCl (4 mol/L in 1,4-dioxane), DCM, 0 °C – r.t., 2 h; (e) phenyl chloroformate, pyridine, DCM, r.t., 12 h; (f) hydroxyl esters or amino esters, DIPEA, THF, $CHCl_3$, reflux, 12 h; (g) LiOH·H_2O, THF, H_2O, r.t., 12 h.

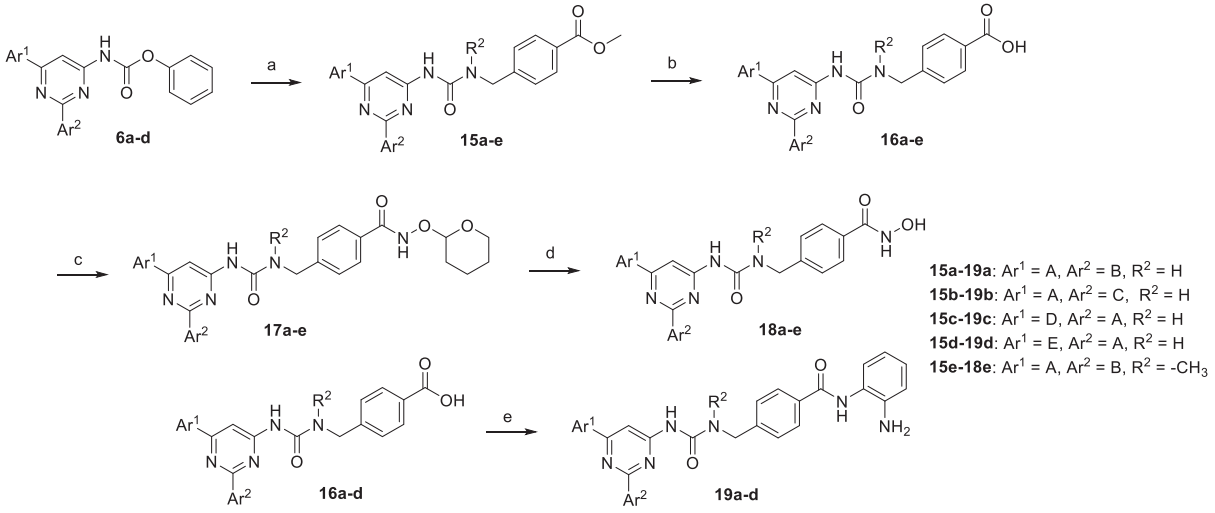

Scheme 2. Synthesis of compounds **18a**-**e** and **19a**-**d**. Reagents and conditions: (a) hydroxyl esters or amino esters, DIPEA, THF, $CHCl_3$, reflux, 12 h; (b) LiOH·H_2O, THF, H_2O, r.t., 12 h; (c) 2-(aminooxy)tetrahydro-2*H*-pyran, HATU, DIPEA, DCM, r.t., 12 h; (d) HCl (4 mol/L in 1,4-dioxane), DCM, 0 °C–r.t., 2 h; (e) *o*-phenylenediamine, HATU, DIPEA, DCM, r.t., 12 h.

Table 2
Antiproliferative activity in cancer cell lines (GI_{50}, μmol/L).[a]

Compound	CT26	MC38	HCT116
5a	2.5 ± 0.2	2.3 ± 0.5	0.15 ± 0.01
5b	8.4 ± 0.8	7.9 ± 1.6	1.92 ± 0.02
5c	9.8 ± 0.9	7.9 ± 1.1	0.63 ± 0.01
5d	8.0 ± 0.7	8.0 ± 1.9	1.8 ± 0.1
5e	4.8 ± 0.1	5.0 ± 0.9	0.74 ± 0.11
5f	13.9 ± 0.3	14.2 ± 4.1	0.21 ± 0.04
5g	28.1 ± 2.5	24.6 ± 4.4	5.2 ± 0.6
10b	8.1 ± 0.3	6.7 ± 1.1	2.9 ± 0.1
10c	3.0 ± 0.4	2.7 ± 0.5	0.17 ± 0.02
10d	2.0 ± 0.4	1.8 ± 0.4	0.22 ± 0.02
10e	6.9 ± 1.3	8.0 ± 1.6	0.44 ± 0.03
10f	19.0 ± 3.9	19.7 ± 5.0	1.33 ± 0.12
10g	12.5 ± 0.1	11.0 ± 2.0	0.62 ± 0.05
10h	8.1 ± 0.5	6.3 ± 1.0	2.7 ± 0.2
10i	4.9 ± 0.4	4.8 ± 0.7	1.2 ± 0.1
14b	14.7 ± 0.7	13.2 ± 1.6	0.74 ± 0.01
14c	6.1 ± 1.1	5.8 ± 1.8	0.21 ± 0.03
14d	11.6 ± 1.7	12.4 ± 3.7	1.3 ± 0.1
18a	2.4 ± 0.3	1.5 ± 0.5	0.25 ± 0.02
18b	7.9 ± 0.8	7.0 ± 0.3	0.90 ± 0.01
18c	9.6 ± 0.3	8.2 ± 2.0	0.51 ± 0.06
18d	>30	>30	7.0 ± 0.1
18e	8.3 ± 1.3	8.7 ± 1.0	0.86 ± 0.04
19b	8.0 ± 0.9	7.9 ± 2.0	0.71 ± 0.13
19c	27.9 ± 1.3	28.1 ± 2.1	3.3 ± 0.2
19d	27.7 ± 0.5	19.6 ± 1.2	2.3 ± 0.2
PBF-509	>30	>30	>30
SAHA	2.4 ± 0.2	2.7 ± 0.1	0.30 ± 0.23
MGCD-0103	2.1 ± 0.3	1.8 ± 0.2	0.53 ± 0.18

[a] Values for $n \geq 2$ reported as the mean ± SEM.

compounds with 2-amino benzamide as the ZBG showed weaker HDAC activity than the hydroxamic acids. Finally, the furyl and pyrazol substituents on the pyrimidine core were replaced with pyridyl and phenyl groups, and appropriate linkers were incorporated to synthesize compounds **10g-i**, **18b-d**, and **19b-d**. The activity of these pyridine and 2-methoxypyridine-containing compounds was slightly better.

The compounds with potent bifunctional activities were tested for their antiproliferative activities against both murine and human colon cancer cell lines (MC38, CT26 and HCT116). The results are shown in Table 2. Because $A_{2A}AR$ antagonists do not possess direct cytotoxicity against the tumor cells *in vitro* [29,30], the antiproliferative activity of these compounds were expected to be correlative to their HDAC inhibition potency. In these assays, compound **PBF-509** showed no observable activity (GI_{50} > 30 μmol/L). Among the dual-acting compounds, **5a**, **10c**, **10d** and **18a** displayed the most potent activity against the three cell lines, being comparable to that of **SAHA** (GI_{50} = 2.7 μmol/L, 2.4 μmol/L and 0.30 μmol/L for MC38, CT26 and HCT116, respectively) and **MGCD-0103** (GI_{50} = 1.8 μmol/L, 2.1 μmol/L and 0.53 μmol/L for MC38, CT26 and HCT116, respectively). These results showed that through the incorporation of HDAC inhibition activity, the bifunctional compounds acquired very potent antiproliferative activity against tumor cells *in vitro*. It worth pointing out that some compounds, for example **18d**, showed very weak antiproliferative activity despite very potent HDAC inhibition. This might be due to their poor permeability properties.

To predict the binding modes of these bifunctional molecules at both $A_{2A}AR$ and HDACs, compound **5a** was selected for molecular docking studies (Fig. 3). The 2-methylfuran substituent of **5a** occupies the hydrophobic pocket, with the dimethylpyrazole substituent fitting into the ribose-binding pocket deeper inside the receptor. In addition, Phe168 on ECL2 forms a π-π stacking interaction with the pyrimidine moiety. Unexpectedly, the hydroxamate group makes H-bonding interactions with the side chain of Asp170

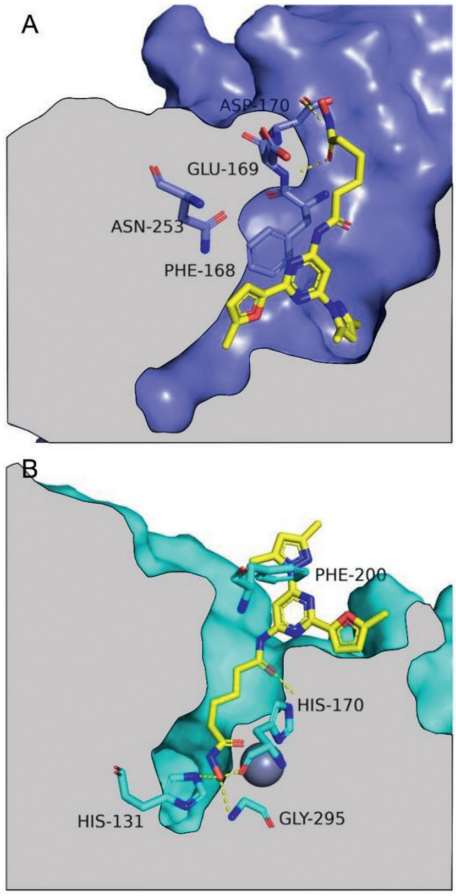

Fig. 3. Binding poses of **5a** in $A_{2A}AR$ and HDAC1 predicted by molecular docking. Compound **5a** is shown in yellow. Key residues interacting with **5a** are highlighted. Nitrogen atoms are colored in blue and oxygen atoms in red. (A) The predicted binding pose of **5a** in $A_{2A}AR$. Structures of $A_{2A}AR$-StaR2-b_{RIL}562 (PDB ID: 6GT3) is shown in deepblue. (B) The predicted binding pose of **5a** in HDAC1. Structures of HDAC1 (PDB ID: 1C3S) is shown in cyan, and the zinc ion is shown as gray sphere.

and the skeleton of Glu169. In HDAC1, the core structure of **5a** lies outside of the binding pocket, with the alkyl chain inserting into the pocket and the hydroxamate group chelating with the zinc ion. The carbonyl group of the amide linker makes an H-bond with the side chain of His170. The hydroxamate group also makes H-bond interactions with the side chains of His131 and Gly295. The trisubstituted pyrimidine core lies on the enzyme surface and forms an edge-to-face π-π interaction with Phe200. These observations predicted the structural basis of the bifunctional activity of our new compounds.

In summary, the incorporation of the key structural element for HDAC inhibition to the solvent-exposed position of $A_{2A}AR$ has culminated the discovery of a series of potent **PBF-509**-derived $A_{2A}AR$/HDAC bifunctional inhibitors. Most compounds displayed nanomolar or subnanomolar inhibitory activity against both $A_{2A}AR$ and HDAC1. In addition, they exhibited equivalent antiproliferative activity to that of **SAHA** and **MGCD-0103** against colon cancer cell lines. Based on the $A_{2A}AR$/HDAC bifunctional activity of these compounds, they are promising leads for further studies as novel tumor immunotherapeutic agents.

Declaration of competing interest

The authors declare that they have no known competing financial interests or personal relationships that could have appeared to influence the work reported in this paper.

Acknowledgments

This work was supported by Lingang Laboratory (No. LG-QS-202205–03), ShanghaiTech University and the Shanghai Municipal Government. We acknowledge Dr. Lingyun Yang for his help in obtaining NMR data.

Supplementary materials

Supplementary material associated with this article can be found, in the online version, at doi:10.1016/j.cclet.2023.108136.

References

[1] J. Blay, T.D. White, D.W. Hoskin, Cancer Res. 57 (1997) 2602–2605.
[2] D. Vijayan, A. Young, M. Teng, et al., Nat. Rev. Cancer 17 (2017) 709–724.
[3] B.B. Fredholm, A.P. Ijzerman, K.A. Jacobson, et al., Pharmacol. Rev. 63 (2017) 1–34.
[4] A. Ohta, M. Sitkovsky, Nature 414 (2001) 916–919.
[5] A. Ohta, E. Gorelik, S.J. Prasad, et al., Proc. Natl. Acad. Sci. U. S. A. 103 (2006) 13132–13137.
[6] J. Kjaergaard, S. Hatfield, G. Jones, et al., J. Immunol. 201 (2018) 782–791.
[7] J. Zhang, W. Yan, W. Duan, et al., Pharmaceuticals 13 (2020) 237.
[8] F. Yu, C. Zhu, Q. Xie, et al., J. Med. Chem. 63 (2020) 12196–12212.
[9] A. Anighoro, J. Bajorath, G. Rastelli, et al., J. Med. Chem. 57 (2014) 7874–7887.
[10] Y. Ren, Q. Sun, Z. Yuan, et al., Chin. Chem. Lett. 30 (2019) 1233–1236.
[11] Q. Sun, Q. Dai, C. Zhang, et al., Chin. Chem. Lett. 32 (2021) 2479–2483.
[12] X. Cai, H.X. Zhai, J. Wang, et al., J. Med. Chem. 53 (2010) 2000–2009.
[13] C.J. Lai, R. Bao, T. Xu, et al., Cancer Res. 70 (2010) 3647–3656.
[14] C. Ding, D. Li, Y.W. Wang, et al., Chin. Chem. Lett. 28 (2017) 1220–1227.
[15] K. Sun, R. Atoyan, M.A. B.orek, et al., Mol. Cancer Ther. 16 (2016) 285–299.
[16] Y. Huang, S. Chen, S. Wu, et al., Acta Pharm. Sin. B 10 (2020) 1294–1308.
[17] S. Wu, Y. Huang, T. Wang, et al., J. Med. Chem. 65 (2022) 4818–4831.
[18] Y. Huang, G. Dong, H. Li, et al., J. Med. Chem. 61 (2018) 6056–6074.
[19] X. Liang, J. Zang, X. Li, et al., J. Med. Chem. 62 (2019) 3898–3923.
[20] W. Yan, L. Ling, Y. Wu, et al., J. Med. Chem. 64 (2021) 16573–16597.
[21] J. Zhang, Z. Luo, W. Duan, et al., Eur. J. Med. Chem. 236 (2022) 114326.
[22] A. Borodovsky, C.M. Barbon, Y. Wang, et al., J. ImmunoTher. Cancer 8 (2020) e000417.
[23] J.A. Camacho Gomez, J.C. Castro-Palomino Laria, Patent, WO2011121418 A1, 2011.
[24] D.H. Slee, Y. Chen, X. Zhang, et al., J. Med. Chem. 51 (2008) 1719–1729.
[25] D. Slee, M. Lanier, B.G. Vong, et al., Patent, WO2006110884 A2, 2006.
[26] D. Slee, X. Zhang, J.K. Rueter, et al., Patent, WO2007084914 A2, 2007.
[27] B. Bernet, P.M. Bishop, M. Caron, et al., Can. J. Chem. 63 (1985) 2818–2820.
[28] M. Mediavilla-Varela, J. Castro, A. Chiappori, et al., Neoplasia 19 (2017) 530–536.
[29] P.A. B.eavis, N. Milenkovski, M.A. H.enderson, et al., Cancer Immunol. Res. 5 (2015) 506–517.
[30] R.D. L.eone, I.M. S.un, M.H. O.h, et al., Cancer Immunol. Immun. 67 (2018) 1271–1284.